Computers and Geotechnics **1** (1985) 161–180

ANALYSIS OF CYLINDRICAL CAVITY EXPANSION IN A STRAIN WEAKENING MATERIAL

J.P. Carter and S.K. Yeung
School of Civil and Mining Engineering
University of Sydney
Sydney, N.S.W., 2006
Australia

ABSTRACT

A numerical technique is suggested that allows a prediction of the behaviour of a single phase, strain softening material during the expansion of a long cylindrical cavity. The method provides the entire pressure-expansion relationship, including the identification of the limit pressure at large deformations.

The numerical solutions, obtained using the finite element technique and allowing for finite deformations, show very good agreement with closed form answers that are available for a restricted class of material models. Results are also presented for the more general, dilatant (or collapsing), strain softening materials for which closed form solutions do not exist. The importance of the rate of dilation and rate of softening in determining the behaviour during cavity expansion is illustrated.

INTRODUCTION

The problem of the expansion of a cylindrical cavity in an ideal soil or rock mass is an important one in the geotechnical engineering. This is because the analysis has applications such as in the interpretation of the pressuremeter test (e.g. Gibson and Anderson, 1961; Ladanyi, 1963, 1972) and predicting the state of stress in the ground around driven piles (e.g. Vesic, 1972; Randolph et al, 1979). In most instances the problem has been idealised as either the expansion of a long cylindrical cavity contained within an infinite, homogeneous, isotropic soil or rock mass. Only in special cases has it been possible to solve the problem analytically (e.g. Chadwick, 1959; Hill, 1950; Gibson and Anderson, 1961; Davis et al, 1984) and so a numerical treatment has often been used, particularly where more realistic constitutive models have been employed (e.g. Carter et al, 1979).

Computers and Geotechnics 0266-352X/85/$03·30

In this paper a numerical method of analysis is presented for the expansion of a long cylindrical cavity in a strain weakening material. As shearing occurs around the cavity the material may either dilate or compress (collapse) and the plastic volume change can be specified to continue indefinitely or to terminate at some nominated plastic shear strain level. The formulation allows the analysis of finite deformations so that predictions can be made of the limit pressures approached during the cavity expansion. Results are presented which show the influence of strain weakening and dilation on the limit pressures for cylindrical cavities in cohesive-fictional materials.

ANALYSIS

In this treatment it is assumed that the deformations in the material around the cavity occur under conditions of plane strain and axial symmetry. This greatly simplifies the analysis and means that a one-dimensional formulation may be used. The displacements in the body are everywhere radial and since large deformations may occur, the radial coordinate of a typical particle may change significantly during the course of the cavity expansion. Because of the possible geometric and material non-linearities associated with this problem, it is convenient to adopt a rate formulation and to use an incremental solution procedure. The basic assumptions of the analysis are listed below.

(1) The cavity expansion is assumed to occur in a medium of infinite extent. Initially, at time t=0, the cavity has a radius a_o and an internal pressure p_o. Everywhere in the surrounding material the radial and circumferential stress components are compressive and have magnitude p_o.

(2) At time t later the cavity radius is a and the internal pressure has increased to a value p. A typical material point of the continuum now has a radial coordinate r, having moved to this position from its original location r_o. The total stress at this position and at this time must be in equilibrium with the current boundary tractions. In the absence of body forces this requirement can be expressed as

$$\frac{\partial \sigma_r}{\partial r} + \frac{\sigma_r - \sigma_\theta}{r} = 0 \qquad (1a)$$

and

$$\sigma_r = p \quad \text{at} \quad r = a \qquad (1b)$$

$$\sigma_r = p_o \quad \text{at} \quad r = \infty \qquad (1c)$$

where σ_r, σ_θ are the normal stress components in a cylindrical

coordinate system. Adopting the convention of compression positive means that during cavity expansion σ_r is the major and σ_θ is the minor principal stress.

(3) The constitutive law for the material of the continuum may be written as a relationship between the rates of change of stress and strain, i.e.

$$\dot{\sigma} = D\,\dot{\varepsilon} \tag{2}$$

where $\dot{\sigma}^T = (\dot{\sigma}_r, \dot{\sigma}_\theta)$

$\dot{\varepsilon}^T = (\dot{\varepsilon}_r, \dot{\varepsilon}_\theta)$

and $\dot{\varepsilon}_r = -\frac{\partial \dot{u}}{\partial r}$

$\dot{\varepsilon}_\theta = -\frac{\dot{u}}{r}$

The symbol u has been used to denote the total radial displacement of a material point in the time interval 0 to t. The dot indicates differentiation with respect to time. Even though displacements may be large, equation (2) is general enough for our purposes here since the kinematic restraints do not permit rotation of principal stress and strain directions. Of course if the cavity is created in a saturated, porous medium then the total stress rate in equation (2) should be replaced by the effective stress rate. For simplicity, attention here shall be restricted to a single phase (dry) soil or rock medium. The coefficients of the matrix D in equation (2) depend on the type of material being analysed. Details shall be given in a later section for an ideal strain weakening soil or rock.

The above assumption can be incorporated into a solution of the cavity expansion problem by applying the principal of virtual work. Hence at time t this can be written in terms of cylindrical components as

$$\int_0^{2\pi}\int_a^{\infty} (\delta\dot{\varepsilon}_r\sigma_r + \delta\dot{\varepsilon}_\theta\sigma_\theta) r\, dr\, d\theta = \int_0^{2\pi} \delta\dot{u}_a p a\, d\theta \tag{3a}$$

or

$$2\pi \int_a^{\infty} \delta\dot{\varepsilon}^T \sigma\, r\, dr = 2\pi a\, \delta\dot{u}_a p \tag{3b}$$

where $\delta\dot{\varepsilon}_r$, $\delta\dot{\varepsilon}_\theta$ are the virtual strain rates and $\delta\dot{u}_a$ is the virtual radial velocity of the cavity wall.

The rate form of the constitutive equation (2) can be integrated over the time interval t-Δt to t, viz

$$\underset{\sim}{\sigma} - \underset{\sim}{\sigma}_{t-\Delta t} = \int_{t-\Delta t}^{t} D\underset{\sim}{\dot{\varepsilon}}\, dt \qquad (4)$$

where $\underset{\sim}{\sigma}_{t-\Delta t}$ is the vector of stress components for the material point now located at radius r but at the previous time $t-\Delta t$.

Substituting equation (4) into equation (3) gives

$$2\pi \int_{a}^{\infty} \delta\underset{\sim}{\dot{\varepsilon}}^{T} \left\{ \int_{t-\Delta t}^{t} D\underset{\sim}{\dot{\varepsilon}}\, dt \right\} r\, dr = 2\pi a \delta u_{a} p - 2\pi \int_{a}^{\infty} \delta\underset{\sim}{\varepsilon}^{T} \underset{\sim}{\sigma}_{t-\Delta t} r\, dr \qquad (5)$$

This is an exact equation governing the behaviour of the body as the cavity is expanded from radius $a-\Delta a$ to a during the time interval $t-\Delta t$ to t.

NUMERICAL SOLUTION

An approximate solution of equation (5) can be obtained using the finite element method. The infinite body is divided into a discrete number of annular elements of finite size, together with an outermost element of infinite extent. 'Nodes' are located at the interfaces between all elements and at the innermost boundary (the cavity wall). The interface between the last annular element and the infinite element can be selected so that the infinite element always remains elastic. Hence its stiffness can always be computed from the theory for a cylindrical cavity expansion in an infinite elastic material.

For the finite region divided into a discrete number (N-1) of conforming annular elements it is supposed that the displacement field can be adequately represented by values at the connecting nodes 1, 2, ..., N. If we let

$$\underset{\sim}{u}^{T} = (u_1, u_2, \ldots, u_N) \qquad (6)$$

then we further suppose that the continuous velocity field $\dot{u}$ can be approximated by

$$\dot{u} = A\underset{\sim}{\dot{u}} \qquad (7)$$

where $A = (N_{11}, N_{12}, N_{21}, N_{22}, \ldots, N_{N1}, N_{N2})$

and N_{ij} = the shape function for the jth node of element i

Hence the strain rates are related to nodal velocities by

$$\underset{\sim}{\dot{\varepsilon}} = B\underset{\sim}{\dot{u}} \qquad (8)$$

where $$B = \begin{bmatrix} -\frac{\partial}{\partial r} \\ -\frac{1}{r} \end{bmatrix} A$$

Substituting into equation (5) it is found that for arbitrary variations $\delta\dot{\underset{\sim}{u}}$ consistent with the velocity boundary conditions

$$\delta\underset{\sim}{u}^T \left[2\pi \int_a^\infty \left\{ B^T \int_{t-\Delta t}^{t} D\, B\, \dot{\underset{\sim}{u}}\, dt \right\} r\, dr - \underset{\sim}{h} \right] = 0 \qquad (9)$$

and thus that

$$2\pi \int_a^\infty \left\{ B^T \int_{t-\Delta t}^{t} D\, B\, \dot{\underset{\sim}{u}}\, dt \right\} r\, dr = \underset{\sim}{h} \qquad (10a)$$

where $$\underset{\sim}{h} = 2\pi \int_a^\infty B^T\, \underset{\sim}{\sigma}_{t-\Delta t}\, r\, dr + 2\pi a p \qquad (10b)$$

Equation (10) is a set of finite element equations which can be solved for the increments of nodal displacement occurring in the time interval t-Δt to t.

CONSTITUTIVE MODEL

The elastoplastic constitutive model used in this treatment requires specification of the following:

(i) a yield function, f

(ii) a flow rule or a plastic potential, g

(iii) a hardening or softening law, and

(iv) a set of elastic constants to describe the elastic behaviour

For purely elastic deformations the constitutive matrix D is given by

$$D = D_E = \begin{bmatrix} \lambda+2G & \lambda \\ \lambda & \lambda+2G \end{bmatrix} \qquad (11)$$

where λ is the Lamè modulus and G is the shear modulus of the material.

The well known matrix equation relating the stress increments $d\underset{\sim}{\sigma}$ (or stress rates) to the strain increments $d\underset{\sim}{\varepsilon}$ (or strain rates) for a strain softening material has the form

$$d\underset{\sim}{\sigma} = \left[I - \frac{D_E\, \underset{\sim}{a}\, \underset{\sim}{b}^T}{\underset{\sim}{b}^T D_E \underset{\sim}{a} - \underset{\sim}{c}^T \underset{\sim}{H} \underset{\sim}{a}} \right] D_E\, d\underset{\sim}{\varepsilon} \qquad (12)$$

where I is the unit matrix, and

$$\underset{\sim}{a} = \frac{\partial g}{\partial \underset{\sim}{\sigma}}$$

$$\underset{\sim}{b} = \frac{\partial f}{\partial \underset{\sim}{\sigma}}$$

$$\underset{\sim}{c} = \frac{\partial f}{\partial h}$$

where $f = f(\underset{\sim}{\sigma},h)$, $g = g(\underset{\sim}{\sigma},h)$ and h is a parameter that defines the nature of the strain weakening. The matrix H relates the strain softening parameter h to the plastic strain components, i.e.

$$dh = H\, d\underset{\sim}{\varepsilon}^P \tag{13}$$

In the present application we postudate a yield function f and a plastic potential g which, when expressed in terms of principal stress components σ_1 and σ_3, are given by

$$f = \sigma_1 - N_\phi \sigma_3 - 2c\sqrt{N_\phi} = 0 \tag{14}$$

$$g = \sigma_1 - N_\psi \sigma_3 - 2c\sqrt{N_\psi} = 0 \tag{15}$$

where $N_\phi = \dfrac{1 + \sin\phi}{1 - \sin\phi}$

$$N_\psi = \frac{1 + \sin\psi}{1 - \sin\psi}$$

Equation (14) is recognisable as the Mohr-Coulomb criterion where c and ϕ are the instantaneous values of cohesion and friction angle, respectively. In the expression (15) for the plastic potential, ψ is the instantaneous angle of dilation giving a flow rule as suggested by Davis (1968). All of the parameters c, ϕ, ψ may be functions of the softening parameter h. Whenever $f = 0$ the material is yielding and perhaps softening, and whenever $f < 0$ it is deforming elastically.

With the above definitions of f and g the vectors $\underset{\sim}{a}$ and $\underset{\sim}{b}$ of equations (12) are given by

$$\underset{\sim}{a}^T = (1, -N_\psi) \tag{16a}$$

$$\underset{\sim}{b}^T = (1, -N_\phi) \tag{16b}$$

It is also postulated that the plastic shear strain $\gamma^P = \varepsilon_1{}^P - \varepsilon_3{}^P$ can be used as a measure of the softening, i.e. $h = \gamma^P$ and hence $H = (1, -1)$. Furthermore, the strength parameters c and ϕ are reduced by an increase in γ^P and the rate of dilation as measured by ψ is also a function of γ^P. Specifically, the following variations are adopted in this paper:

(a) when $0 \leq \gamma^P \leq \gamma_c^P$

$$c = c_p - (c_p - c_r)\frac{\gamma^P}{\gamma_c^P} \tag{17}$$

$$\tan\phi = \tan\phi_p - (\tan\phi_p - \tan\phi_r)\frac{\gamma^P}{\gamma_c^P} \tag{18}$$

$$\psi = \psi_o \tag{19}$$

(b) when $\gamma^P > \gamma_c^P$

$$c = c_r \tag{20}$$

$$\tan\phi = \tan\phi_r \tag{21}$$

$$\psi = 0$$

These assumptions define a peak response, at which point $c = c_p$, $\phi = \phi_p$, followed by a period of strain softening and then eventually (when $\gamma^P > \gamma_c^P$) a residual strength behaviour. The postpeak softening is linear in the accumulated plastic shear strain γ^P. During the softening period the material dilates at a constant rate and the cohesive component of strength is gradually diminished while the friction component is simultaneously reduced. In general the possibility of a non-zero residual cohesion intercept has been included in the model. This has been found to be significant in some naturally occuring cemented materials because of the presence of silt and clay particles. At a specified magnitude of plastic shear strain γ_c^P, a residual behaviour is reached at which point the material has constant strength defined by $c = c_r$ and $\phi = \phi_r$. Once the residual behaviour is reached there is no further plastic volume change. This behaviour is illustrated schematically in Fig.1 for a single element of the material undergoing a simple shear deformation. A model similar to this has been proposed for strain weakening materials by Simmons (1981).

Because the hardening parameter has been defined as $h = \gamma^P$, the vector $\underset{\sim}{c}$ of the equation (12) can now be determined from

$$\underset{\sim}{c} = \frac{\partial f}{\partial h} = \frac{\partial f}{\partial \gamma^P} = \frac{\partial f}{\partial c}\frac{\partial c}{\partial \gamma^P} + \frac{\partial f}{\partial N_\phi}\frac{\partial N_\phi}{\partial \gamma^P} \tag{23}$$

The explicit form of this equation, together with equations (16a and b) can then be substituted into equation (12) to determine explicitly the incremental stress-strain law.

For this ideal material, softening must be accompanied by an increase in plastic work. This is possible as long as

$$\underset{\sim}{b}^T \underset{E}{D} \underset{\sim}{a} - \underset{\sim}{c}^T \underset{\sim}{H} \underset{\sim}{a} > 0 \qquad (24)$$

This relation imposes a restriction on the rate of softening, i.e. there will be a limit on the magnitude γ_c^P required for stable softening.

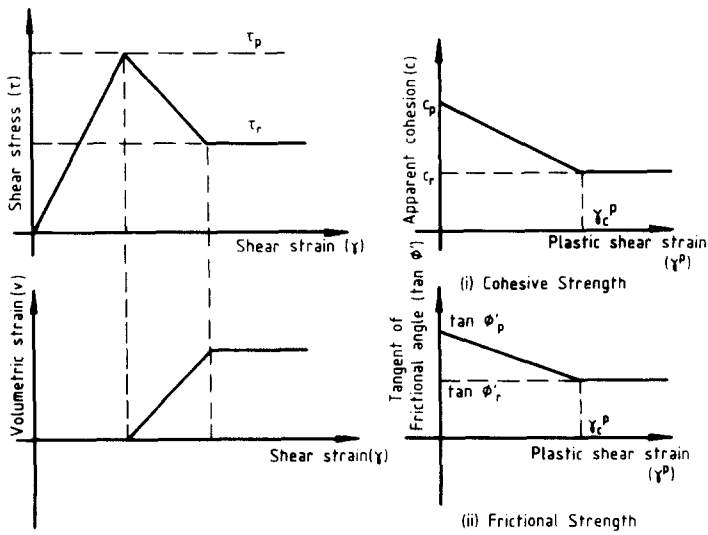

FIG. 1(a) STRESS-STRAIN BEHAVIOUR FOR AN IDEALISED STRAIN-SOFTENING MATERIAL

FIG. 1(b) STRENGTH REDUCTION IDEALISATION DURING SOFTENING

PARAMETER DETERMINATION

Eight parameters are required to completely determine the behaviour of the ideal strain weakening material. These are: the elastic moduli λ and G; strength parameters c_p, c_r, ϕ_p, ϕ_r; the dilation angle ψ; and γ_c^P, the parameter which determines the rate of softening. Ideally these values should be measured in the laboratory (or the field) under conditions of plane strain deformation if they are to be applied to the problem of cylindrical cavity expansion. However, plane strain tests are somewhat rare and are usually confined to the research environment. A much more common means of determining strength and deformation parameters in the laboratory is with the triaxial apparatus. It is suggested that values for all the material parameters may be obtained from conventional triaxial compression tests, but it must further be assumed that values determined under triaxial conditions are also appropriate for the plane strain case. This may not be strictly correct, but the values obtained should give a guide to the role that material softening plays in the behaviour during cavity expansion.

Results of fully drained triaxial compression tests are often represented as plots of deviator stress $\sigma_1-\sigma_3$ versus axial strain ε_1 and volumetric strain $v = \varepsilon_1 + 2\varepsilon_3$ versus axial strain. Such plots allow values of the elastic properties λ, G (or E and ν) to be determined from the initial slopes of the curves. The rate of dilation, as defined in equation (15), can be determined from the $v - \varepsilon$, curve and this task is made relatively simple if the elastic components of the total strain are assumed to be small and thus ignored. The onset of the residual condition can usually be determined from these plots if during testing, the straining is allowed to continue for long enough beyond the peak condition. From this an estimate can be made of ε_1 and ε_3 at the residual condition and hence $\gamma_c{}^p$ can be calculated. Finally, the strength parameters can be determined from the Mohr circle plots corresponding to the peak and residual conditions from a series of tests on the material.

VALIDATION OF THE METHOD

The method of analysis outlined above can be used to obtain the complete cavity pressure - wall displacement relationships as well as the stress distribution throughout the body at any stage of the expansion. An estimate of the limit pressure, i.e. the pressure required to enlarge the cavity indefinitely, can be obtained if the analysis is allowed to continue long enough for a pressure asymptote to be numerically identified. In this section, some numerical results will be described and compared with available analytical solutions to illustrate the accuracy of the proposed technique.

Perfectly Plastic Materials

Two basic assumptions that are often made in order to obtain closed form solutions to the expansion problem are:

(i) that shearing takes place under condition of no volume change (i.e., $\nu = 0.5$ and $\psi = 0$), and

(ii) that the material behaves in an elastic and perfectly plastic fashion, i.e. it does not strain harden or soften.

Of course, materials behaving in this manner form a special case of the more general class of softening materials described previously, but closed form solutions for cavity expansions in this more restricted class of materials provide a means of checking the numerical solution procedure.

The results of a numerical analysis for a material characterised by $\phi = \psi = 0$, $c = c_u$, where c_u is a constant, $G/c_u = 50$ and $\nu = 0.49$ are

given in Fig.2. Figure 2 shows the increase in cavity pressure above its initial value $p-p_o$, normalised by c_u and plotted against the current cavity radius a, which has been normalised by its initial value a_o. The pressure expansion curve is in good agreement with the well known solution published by Gibson and Anderson (1961) and at large deformations the numerical solution approaches closely the limit pressure derived earlier by Hill (1950).

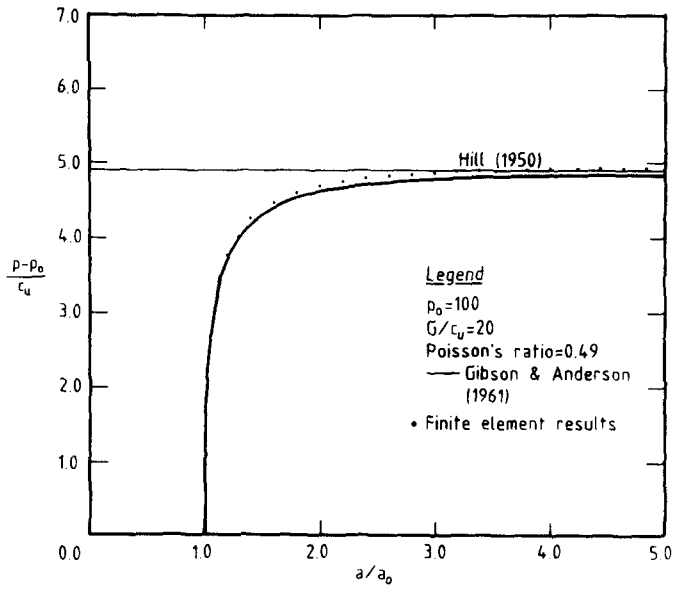

FIG. 2 UNDRAINED CAVITY EXPANSION IN A PURELY COHESIVE MATERIAL

It is also possible to deduce a closed form solution for the cylindrical cavity expansion in a purely frictional material (c=0), as long as the material deforms at constant volume (ν=0.5, ψ=0). The analysis in this case follows the same lines as the original Gibson and Anderson treatment for the purely cohesive material. In Figs.3 and 4 numerical results are presented for the case in which $c = \psi = 0$, $\phi = 30°$, $\nu = 0.49$ ($\approx$0.5) and $G/p_o = 100$ where p_o is the initial in situ hydrostatic pressure. In Fig.3 the pressure increment $p-p_o$, normalised by p_o is plotted against the current non-dimensional cavity size a/a_o. The numerical results show good agreement with the closed form solution and at large expansions they approach the theoretical limit pressure p_L which, incidentally, was also determined independently by Vesic (1972). Figure 4 shows a comparison of the finite element and closed form solutions for the

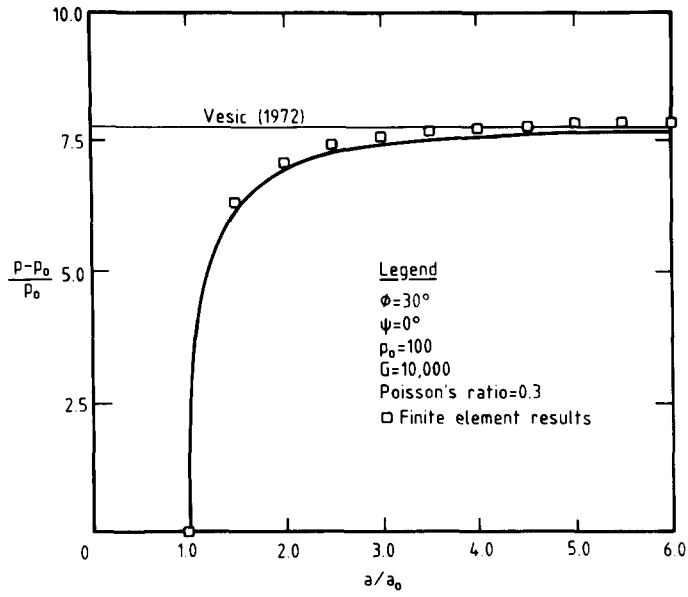

FIG. 3 CAVITY EXPANSION IN A PURELY FRICTIONAL INCOMPRESSIBLE MATERIAL

radial stress distribution at $a/a_o = 5$ and here also the agreement is good. The non-dimensional distribution plotted here shows σ_r normalised by the current cavity pressure p versus the radius r normalised by the current cavity size a. In this form the distribution is valid for all stages of the expansion which involve plastic yielding, because theoretically the radius of the elastic-plastic interface R is always related to the current cavity radius a and internal pressure p by

$$\left(\frac{R}{a}\right)^{\alpha} = \left(\frac{p}{\sigma_R}\right) \tag{26}$$

where $\sigma_R = (1 + \sin\phi)p_o$

$$\alpha = \left(\frac{N_\phi - 1}{N_\phi}\right),$$

and within the plastic zone the radial stress distribution is given by

$$\left(\frac{\sigma_r}{\sigma_R}\right) = \left(\frac{R}{r}\right)^{\alpha} \tag{27}$$

Equations (26) and (27) follow from the equilibrium and yield conditions.

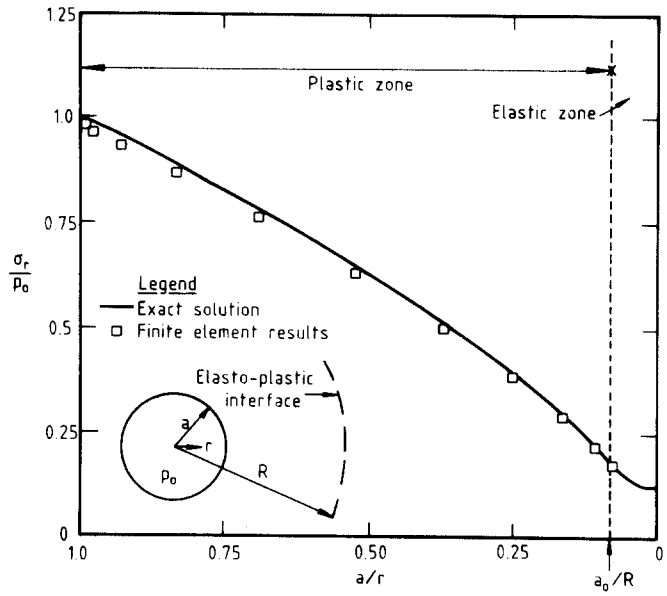

FIG. 4 RADIAL STRESS DISTRIBUTION ($a/a_o=5$)

Softening Materials

It is difficult, if not impossible in some cases, to obtain closed form solutions for cavity expansions in strain softening material. However, Ladanyi (1965), in studying the effects of strain weakening on the expansion of cylindrical cavities in undrained sensitive clays, has been able to obtain an exact solution for the limit pressure in a purely cohesive material deforming under constant volume conditions. The material model as proposed by Ladanyi is indicated in the inset to Fig.5. In terms of the model proposed in this paper it requires $\phi = \psi = 0$, $\nu = 0.5$ and $c = c_u$ with at the peak condition $c_u = c_{up}$ and at residual $c_u = c_{ur}$. In the present case the ratio of residual to peak undrained shear strength was adopted as $c_{ur}/c_{up} = 0.45$, with the peak and residual conditions being attained at total shear strain values of 0.6% and 18.75%, respectively. The ratio of shear modulus to peak undrained shear strength adopted was $G/c_{up} = 167$.

Figure 5 shows a plot of the increase in non-dimensional cavity pressure $(p-p_o)/c_{up}$ versus the non-dimensional cavity size a/a_o. The numerical pressure-expansion curve approaches a limit of 195 which is in excellent agreement with Ladanyi's result of 194.

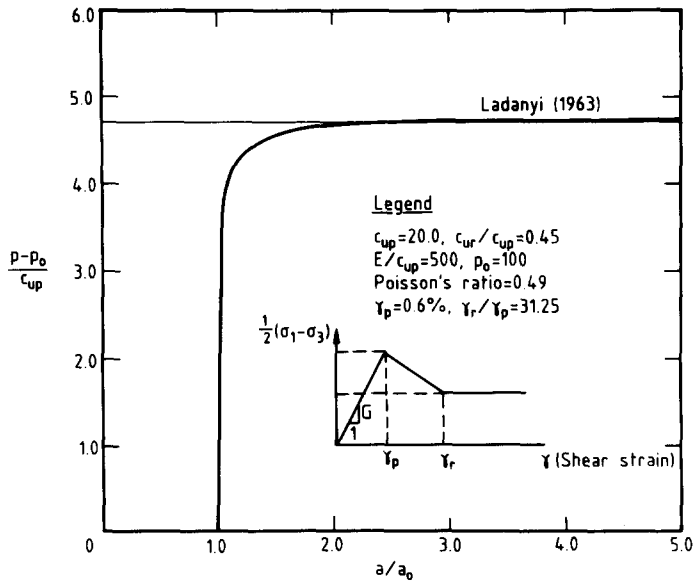

FIG. 5 UNDRAINED CAVITY EXPANSION IN SENSITIVE CLAY

SELECTED NUMERICAL RESULTS

A selection of numerical results is now presented in order to indicate the range of material types for which the proposed analysis may be used and also to briefly indicate the effects of various key parameters on the behaviour during cavity expansion.

Cohesionless Materials

Consider the case of a perfectly plastic, cohesionless material for which ϕ = 30° (i.e. c = 0 and $\phi_p = \phi_r = \phi$). It might be reasonable to model a clean sand in this way, assigning to it an appropriate value for the angle of dilation ψ. Various analyses have been performed for a number of purely frictional materials possessing different dilation rates, viz. ψ = -20°, -10°, 0°, 10°, 20° and 30°. The first two values correspond to materials which collapse volumetrically as plastic shearing takes place, ψ = 0 corresponds to a plastically incompressible material, and positive values of ψ indicate dilatant materials. For these calculations it has been assumed that dilation (or collapse) occurs indefinitely once plastic yielding is initiated (i.e. $\gamma_c^p \rightarrow \infty$) and that the ratio of shear stiffness to the initial hydrostatic stress is G/p_o = 100. A value of 0.3 has been assigned to Poisson's ratio.

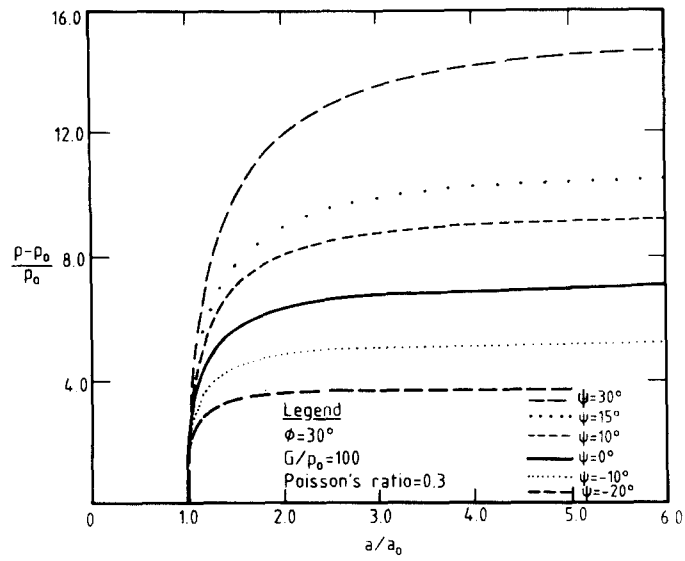

FIG. 6 PRESSURE - EXPANSION CURVES FOR PURELY FRICTIONAL MATERIAL

The pressure-expansion curves for these materials are shown in Fig.6 and the limit pressures p_L is identified for each case have been plotted against dilation angle ψ in Fig.7. In each case the pressures have been normalised by the initial in situ value p_o. It can be observed that for this class of materials the plastic volumetric behaviour has a strong influence on the limit pressure. As the angle of dilatancy decreases and becomes negative the limit pressure drops. For the extreme case with $\psi = -20°$ the limit pressure is about 40% below that for the plastically incompressible material. At the other extreme investigated with $\psi = 30°$ (normality), the limit pressure is about two times that for the incompressible case.

Consider now the case of purely frictional materials which also soften. The results plotted in Fig.8 indicate the effects of the rate of softening on cohesionless materials for which $\phi_p = 30°$, $\phi_r = 10°$, $\psi = 0$ (no dilatancy), $G/p_o = 100$ and $\nu = 0.3$. A number of softening rates have been included covering the range from $\gamma_c^p = 0.01$, which indicates very brittle behaviour, to $\gamma_c^p = \infty$ which corresponds to perfectly plastic, ductile behaviour. Values of γ_c^p between these values indicate intermediate degrees of brittleness. The values of cavity pressure plotted in Fig.8 have been normalised by the limit pressure corresponding to the

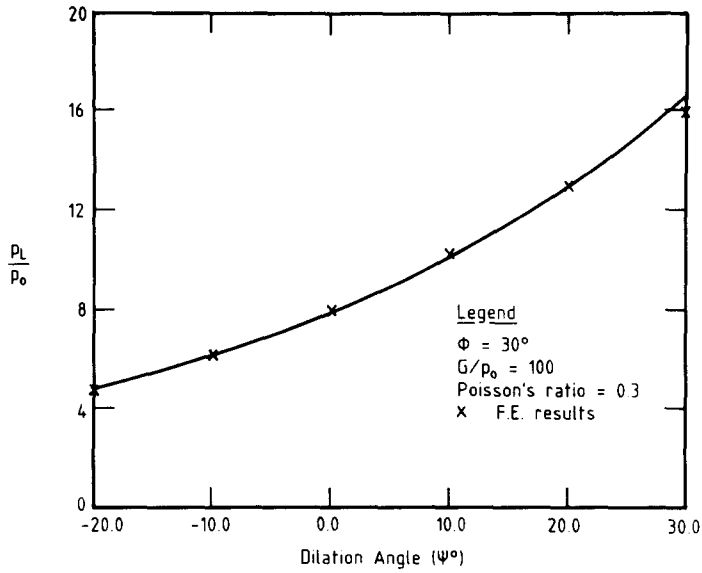

FIG.7 LIMIT PRESSURE FOR A PURELY FRICTIONAL MATERIAL

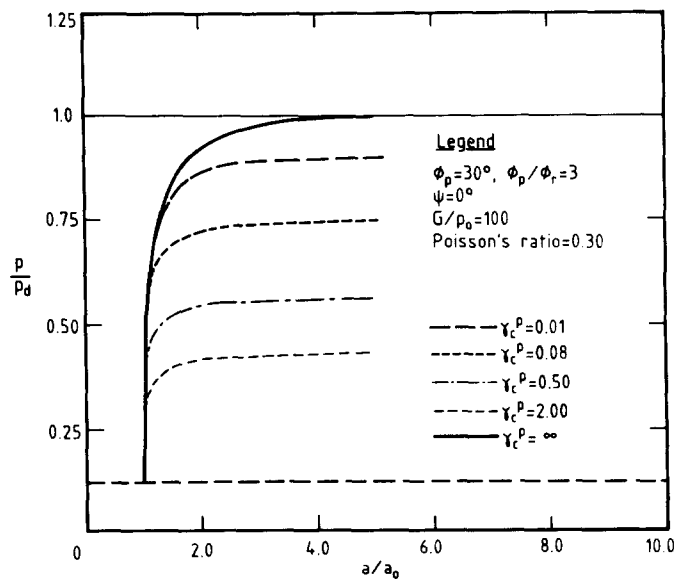

FIG. 8 CAVITY EXPANSION FOR STRAIN - SOFTENING PURELY FRICTIONAL MATERIAL

perfectly plastic, ductile case p_d. Of significance is the effect that the rate of softening (as measured by γ_c^p) has on the limit pressure for this class of materials; the more brittle the material then the lower is the limit pressure. Clean dense sand might typically have a value of γ_c^p in the range 0.15 to 0.20 and for this type of material the reduction in the limit pressure due to strain softening might be up to 40%.

Cohesive-Frictional Materials

An example of the analysis for a purely cohesive material was given earlier in Fig.2 so an illustration will be given here of the more general class of materials possessing both cohesion and friction.

Clough et al (1981) reported a series of laboratory tests on cemented sands found in the San Francisco Bay area and the results suggested that the strongly cemented material tended to have a high peak cohesive strength as well as a small degree of residual cohesion. The friction angle was similar to that of uncemented sands with very little difference between the peak and residual values. A set of parameters was chosen so that the softening model would simulate a deposit of cemented sand and these are c_p = 143 kPa, c_r = 0, $\phi_p = \phi_r$ = 35°, ψ = 15°, G = 80,000 kPa, ν = 0.3 and γ_c^p = 0.08. The initial hydrostatic pressure in the deposit was assumed to be 250 kPa.

These values indicate that as a result of strain softening the entire cohesive component of strength is eventually eliminated but there is no difference in the peak and residual friction angles. Figure 9 shows the cavity expansion curves for the softening material predicted by the finite element analysis. Also shown on this figure are the curves for two perfectly plastic materials which have been assigned constant strength parameters, in one case the same as the peak values and in the other the same as the residual values for the softening material. It is interesting to note that the curve for the softening material lies close to that for the perfectly plastic material assigned the residual strength values. This indicates that the peak cohesion is contributing little to the limit pressure of the softening material. On the other hand if the cohesion is not destroyed during expansion then the limit pressure is significantly greater than for the softening material.

Stress Path for a Softening Material

In the previous examples we have studied the relationships between

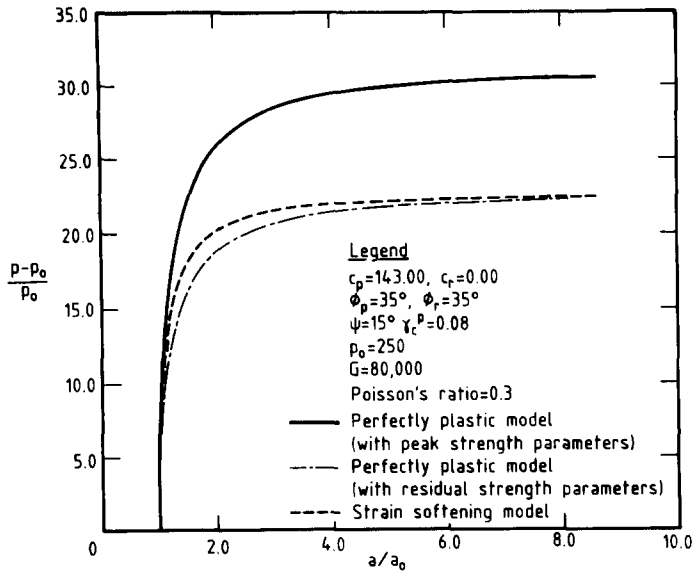

FIG. 9 CAVITY EXPANSION FOR A CEMENTED MATERIAL

internal cavity pressure and the radial displacement of the cavity wall. The influence of various parameters on the limit presssure has also been discussed. However, it is of some interest to investigate the stress path as well as the stress-strain curve followed by a typical element during the cavity expansion.

Consider the case of a purely frictional, collapsing material characterised by the parameters $G/p_o = 100$, $\nu = 0.3$, $\phi_p = 30°$, $\phi_r = 6°$, $\psi = -20°$ and $\gamma_c^p = 2.0$. Such a material undergoes a severe reduction in strength and a large collapse in volume over quite a large range of deformation. It is unlikely that many real materials could be so severely affected by plastic softening, but the choice of these parameters allows a graphic illustration of the softening process.

The stress path and stress-strain relations for a material element immediately adjacent to the cavity wall is shown in Fig. 10. Before discussing these specifically it should be noted that all elements of the medium will follow identical paths, but at any instant during the cavity expansion elements closer to the cavity wall will be further along the path than elements further out in the infinite medium. Fig. 10a shows the stress path plotted in s, t space, where $s = 1/2(\sigma_r + \sigma_\theta)$ and $t = 1/2(\sigma_r - \sigma_\theta)$. All stress values on this figure have been normalised by initial hydrostatic pressure p_o. The initial condition is represented by

point O and during the early expansion the material behaves elastically and deformation occurs at a constant value of s. At point A the material first yields, with its strength determined by the peak friction angle ϕ_p = 30°. As the cavity is further expanded and plastic yielding continues the mean stress s always increases. During the early stages of yielding the deviator stress t also increases even though the friction strength parameter ϕ is steadily reducing with plastic yield. From A the path moves almost along the peak strength envelope for a time* and the stress t reaches a peak value at point B and then reduces. At point C on Fig. 10a the softening process is complete and the material behaves in a perfectly plastic manner with the residual value of friction angle ϕ_r. In this example the arrival at point C of material adjacent to the cavity wall is almost coincident with the attainment of the limit pressure for the cavity expansion. Hence there is little movement along the stress path beyond point C. This may not be true in general, however, and in other cases the stress path will then be restricted to movement along the residual strength envelope until the limit condition is reached.

The stress-strain behaviour for this example is shown as a plot of t versus $\gamma = \varepsilon_r - \varepsilon_\theta$ in Fig. 10b where, for convenience, the reference points O, A, B, C have also been plotted. It can be seen that first yield occurs at point A but this is not the peak in the stress-strain curve. The curve continues to rise as the material deforms plastically until point B is reached. Between B and C the curve falls and beyond C a near horizontal plateau is observed indicating that the softening process has ceased at about the same time that the limit pressure is reached within the cavity. Perfectly plastic deformation of the material element then occurs. For completeness the relation between the volume strain $\varepsilon_r + \varepsilon_\theta$ and the shear strain $\varepsilon_r - \varepsilon_\theta$ for this element is plotted in Fig. 10c. The overall cavity pressure-expansion curve is given in Fig. 10d.

CONCLUSIONS

A technique has been suggested that allows a prediction of the behaviour of a single phase, strain softening material during the expansion

---

* In the plot of Fig. 10a the stress path is shown as being slightly above the peak strength envelope from point A. This is artificial and has arisen because of numerical error causing a slight "overshoot" of the envelope on first yield.

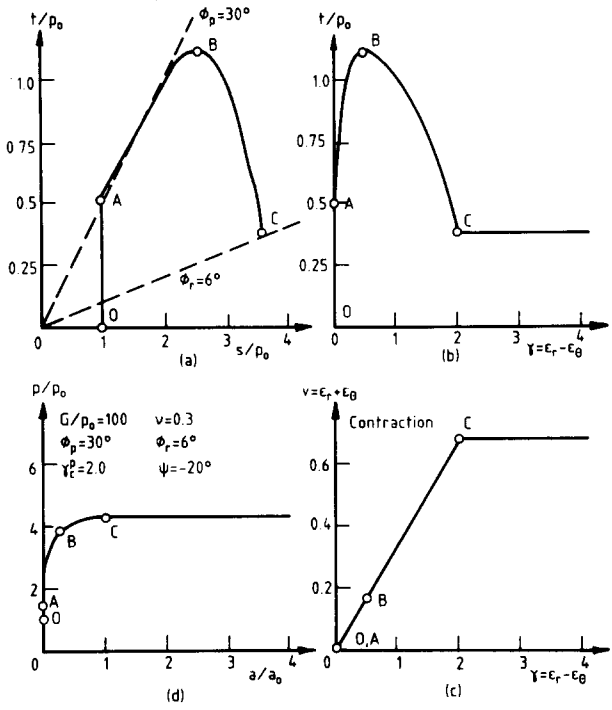

FIG. 10 DETAILS OF CAVITY EXPANSION IN A SOFTENING, COLLAPSING MATERIAL

of a long cylindrical cavity. The method provides the entire pressure-expansion relationship including the identification of the limit pressure at large deformations. It is suggested that the behaviour of a shrinking cylindrical cavity in strain softening material may also be analysed with the current method. Although not persued in this paper the latter solutions would be relevant to the modelling of ground behaviour following a tunnel excavation or a borehole drilling.

For the expansion problem the numerical solutions showed very good agreement with closed form answers that are available for a restricted class of material models. For the more general, dilantant (or collapsing), strain softening materials no such closed form solutions exist and the present numerical technique has been useful in identifying limit pressures and for illustrating the importance of the rate of dilation and the rate of softening on these pressures. The limit pressures may be used in the determination of stress changes around driven piles and the overall response may be helpful in the interpretation of the pressuremeter test.

It is proposed to present a detailed parametric study of the cavity expansion problem in a future paper.

REFERENCES

1. Carter, J.P., Randolph, M.F. and Wroth, C.P.
Stress and pore pressure changes in clay during and after the expansion of a cylindrical cavity. Int. J. Numer. Anal. Methods Geomech. **3** (1979) 305-322.

2. Chadwick, P.
The quasi-static expansion of a spherical cavity in metals and ideal soils. Quarterly Journal of Mechanics and Applied Mathematics **12** (1959) 52-71.

3. Clough, G.W., Star, N., Bochus, R.C. and Rad, N.S.
Cemented sand under static loading. Geotech Engg Divn, ASCE, **107** (1981) 799-817.

4. Davis, E.H.
Theories of plasticity and the failure of soil masses. In: Soil Mechanics Selected Topics Ed. by I.K. Lee, Butterworths, London (1968) 341-380.

5. Davis, R.O., Scott, R.F. and Mullenger, G.
Rapid expansion of a cylindrical cavity in a rate-type soil. Int. J. Numer. Anal. Methods Geomech. **8** (1984) 125-140.

6. Gibson, R.E. and Anderson, W.F.
In-situ measurement of soil properties with the pressurementer. Civil Eng. and Public Works Review **56** (1961) 615-618.

7. Hill, R. The Mathematical Theory of Plasticity, Oxford University Press, London (1950).

8. Lananyi, B.
Evaluation of pressuremeter tests in granular soils. Proc. 2nd Panam. Conf. on Soil Mechanics, San Paulo, 1 (1963) 3-20.

9. Ladanyi, B.
In-situ determination of stress-strain properties of sensitive clays with the pressuremeter. Canadian Geotech. J. **9** (1972) 313-319.

10. Ladanyi, B.
Bearing capacity of deep footings in sensitive clay. Proc. Eighth Int. Conf. Soil Mechanics and Fdn. Engg, Moscow, 2.1 (1973) 159-166.

11. Randolph, M.F., Carter, J.P. and Wroth, C.P.
Driven piles in clay - the effects of installation and subsequent consolidation. Géotechnique. **29** (1979) 361-393.

12. Simmons, J.V.
Shearband yielding and strain weakening, Thesis presented to the University of Alberta, Edmonton, Canada (1981), in partial fulfillment of the requirements for the degree of Doctor of Philosophy.

13. Vesic, A.S.
Expansion of Cavities in Infinite Soil Mass. J. Soil Mech. Fdns, ASCE **98** (1972) 265-290.